

LRFTubes documentation - v1.0

Dr.ir. J.A. de Jong

October 24, 2018



ASCEE
Vildersveenweg 19
7443 RZ Nijverdal
The Netherlands
T: +31 6 18971622
E: info@ascee.nl

Internal document ID:	628318
Document status:	Draft
Document revision:	1
Revision history:	2018-02-21: rev. 1

Copyright (©) 2018 ASCEE. All rights reserved.

Contents

Contents	2
List of symbols	3
1 Overview of LRFTubes	5
1.1 Introduction	5
1.2 License and disclaimer	5
1.3 Features	5
1.3.1 Limitations and future features	6
1.3.1.1 Ducts with (turbulent) flow	6
1.3.1.2 Porous acoustic absorbers	6
1.4 Overview of this documentation	6
2 The transfer matrix method	7
2.1 Introduction	7
2.2 Example transfer matrix of an acoustic duct	7
2.3 Setting up the system of equations	8
3 Provided acoustic models	10
3.1 Introduction	10
3.2 Prismatic duct	10
3.3 Prismatic lined circular duct	12
3.3.1 Cremers impedance	13
3.3.2 Locally reacting lining with back-volume	13
3.4 Compliance volume	13
3.5 End corrections and discontinuities	14
3.6 Hard wall	15
Bibliography	17
A Thermal relaxation in thick tubes	18
A.1 Thermal relaxation effect in thick tubes	18
B Derivation of Karal's discontinuity factor	20
B.1 Boundary conditions	21

List of symbols

Roman symbols

ℓ	Characteristic length scale of a fluid space	[m]
\mathbf{n}	Normal vector pointing from the solid into the fluid	[-]
\mathbf{r}	Transverse position vector	[-]
\mathbf{u}	Velocity vector	[m·s ⁻¹]
\mathbf{x}	Position vector	[m]
a	Tube radius	[m]
c	Speed of sound	[m·s ⁻¹]
C_c	Acoustic capacitance of a compliance volume	[m ³ ·Pa ⁻¹]
c_p	Specific heat at constant pressure	[J·kg ⁻¹ ·K ⁻¹]
c_s	Specific heat of the solid	[J·kg ⁻¹ ·K ⁻¹]
c_v	Specific heat at constant density	[J·kg ⁻¹ ·K ⁻¹]
D	Diameter	[m]
e	Thermal effusivity	[J·m ⁻² ·K ⁻¹ ·s ^{-½}]
f	Frequency	[Hz]
f_k	Thermal Rott function	[-]
f_v	Viscous Rott function	[-]
i	Imaginary unit	[-]
j	Index, subscript placeholder	[-]
J_α	Bessel function of the first kind and order α	
k	Wave number	[rad·m ⁻¹]
L	Length	[m]
M_A	Acoustic mass	[kg·m ⁻⁴]
N	Number of	[-]
N	Number	[-]
p	Pressure, acoustic pressure	[Pa]
r	Radial position in cylindrical coordinates	[m]
r_h	Hydraulic radius	[m]
S	Cross-sectional area, surface area	[m ²]
T	Temperature	[K]
t	Time	[s]
U	Volume flow	[m ³ ·s ⁻¹]
u	Velocity in wave propagation direction	[m·s ⁻¹]
V	Volume	[m ³]

Z	Volume flow impedance	$[\text{Pa}\cdot\text{s}\cdot\text{m}^{-3}]$
z	Specific acoustic impedance	$[\text{Pa}\cdot\text{s}\cdot\text{m}^{-1}]$

Greek symbols

α	Ratio of tube radii	$[-]$
χ	Karal's discontinuity factor	$[-]$
δ_κ	Thermal penetration depth	$[\text{m}]$
δ_ν	Viscous penetration depth	$[\text{m}]$
ϵ_s	Ideal stack correction factor	$[-]$
Γ	Viscothermal wave number for a prismatic duct	$[\text{rad}\cdot\text{m}^{-1}]$
γ	Ratio of specific heats	$[-]$
λ	Wavelength	$[\text{m}]$
Π	Wetted perimeter (contact length between solid and fluid)	$[\text{m}]$
π	Ratio of the circumference to the diameter of a circle	$[-]$

Miscellaneous symbols and operators

\bullet	Placeholder for an operand	
\Im	Imaginary part	
$\ \bullet\ $	Euclidian norm	
∇	Gradient	$[\text{m}^{-1}]$
∇^2	Laplacian	$[\text{m}^{-2}]$
∂	Infinitesimal	
\Re	Real part	
\sim	Same order of magnitude	
d	Infinitesimal	

Abbreviations and acronyms

Eq(s).	Equation(s)
LRF	Low Reduced Frequency
Sec(s).	Section(s)

Sub- and superscripts

f	Fluid
i	Inner
L	Left side
o	Outer
R	Right side
s	Solid
s	Squeeze
t	Tube
w	Wall
0	Evaluated at the reference condition
wall	At the wall

Chapter 1

Overview of LRFTubes

1.1 Introduction

Welcome to the documentation of **LRFTubes**. **LRFTubes** is a numerical code to solve one-dimensional acoustic duct systems using the transfer matrix method. Segments can be connected to generate simple one-dimensional acoustic systems to model acoustic propagation problems in ducts in the frequency domain. Viscothermal dissipation mechanisms are taken into account such that the damping effects can be modeled accurately, below the cut-on frequency of the duct. For more information regarding the models and the theory behind the models, the reader is referred to the work of [3], [4] and [11].

This documentation serves as a reference for the implemented models. For examples on how to use the code, please take a look at the example models as worked out in the IPython Notebooks. For installation instructions, please refer to the [README](#) in the main repository.

This document is very brief on the theory and it is assumed that the reader has some knowledge on the basics of acoustics in general and viscothermal acoustics as well. If you are not falling in this category, I would please refer you first to the book of Swift [9]. A more detailed introduction to the notation used in this documentation can be found in the PhD thesis of de Jong [2].

Besides that, if you find the work interesting, but you are not sure how to apply it, please contact ASCEE for more information.

1.2 License and disclaimer

Redistribution and use in source and binary forms are permitted provided that the above copyright notice and this paragraph are duplicated in all such forms and that any documentation, advertising materials, and other materials related to such distribution and use acknowledge that the software was developed by the ASCEE. The name of the ASCEE may not be used to endorse or promote products derived from this software without specific prior written permission.

THIS SOFTWARE IS PROVIDED “AS IS” AND WITHOUT ANY EXPRESS OR IMPLIED WARRANTIES, INCLUDING, WITHOUT LIMITATION, THE IMPLIED WARRANTIES OF MERCHANTABILITY AND FITNESS FOR A PARTICULAR PURPOSE.

1.3 Features

Currently the **LRFTubes** code provides acoustic models for the following physical entities:

- Prismatic ducts with circular cross section,
- Prismatic ducts with triangular cross section,
- Prismatic ducts with parallel plate cross section,
- Prismatic ducts with square cross section,
- Acoustic compliance volumes

- Discontinuity correction
- End correction for a baffled piston
- Lumped series impedance

These segments can be connected to form one-dimensional acoustic systems to model wave propagation below the cut-on frequency of higher order modes. For a circular cross section, the cut-on frequency is [3]:

$$f_c \approx \frac{c_0}{3.4r}, \quad (1.1)$$

where r is the tube radius and c_0 is the speed of sound. Above the cut-on frequency, besides evanescent waves, there are also propagating waves with a non-constant pressure distribution along the cross section of the duct.

1.3.1 Limitations and future features

The current version of has some limitations that will be resolved in a future release. These are:

1.3.1.1 Ducts with (turbulent) flow

For thermoacoustic and HVAC (Heating, ventilation and Air Conditioning) duct modeling it is imperative that mean flows can be taken into account. An acoustic wave superimposed on a mean flow results in asymmetric wave propagation. More specifically, the phase velocity is higher in the direction of the mean flow, and slower in the opposite direction. In a future release, we will provide models for ducts including a mean flow.

1.3.1.2 Porous acoustic absorbers

To model absorption of sound, a one-dimensional porous material model should be implemented. This work has been postponed to a later stage.

1.4 Overview of this documentation

The next chapter of this documentation will describe the basic framework of the **LRFTubes** code: the transfer matrix method. After that, in Chapter 3, an overview of the provided acoustic models is given, with which acoustic networks can be built. For each of the segments, the resulting transfer matrix model is derived.

Chapter 2

The transfer matrix method

2.1 Introduction

Each part of an acoustic system in **LRFTubes** is modeled using a so-called transfer matrix. A transfer matrix maps the state quantities on one side of the segment (node) to the other side of the segment (node).

For one-dimensional wave propagation, analytical solutions for the velocity, temperature and density field in the transverse direction can be found. The state variables in frequency domain satisfy a system of first order ordinary differential equations. Once the solution is known on one end of a segment, the solution on the other end can be deduced. The transfer matrix couples the state variables ϕ on one end of a segment to the other end, in frequency domain:

$$\phi_R(\omega) = T(\omega)\phi_L(\omega) + \mathbf{s}(\omega), \quad (2.1)$$

where L and R denote the left and right side, respectively, T denotes the transfer matrix and \mathbf{s} is a source term. In the code and in this documentation $e^{+i\omega t}$ convention is used. A common choice of state variables is such that their product has the unit of power. For the acoustic systems in this work the state variables are acoustic pressure $p(\omega)$ and volume flow $U(\omega)$. The acoustic power flow can then be computed as:

$$E = \frac{1}{2} \Re [pU^*], \quad (2.2)$$

where $\Re[\bullet]$ denotes the real part of \bullet , and $*$ denotes the complex conjugation.

2.2 Example transfer matrix of an acoustic duct

This section will provide the derivation of the transfer matrix of a simple acoustic duct. Starting with the isentropic acoustic continuity and momentum equation :

$$\frac{1}{c_0^2} \frac{\partial \hat{p}}{\partial \hat{t}} + \rho_0 \nabla \cdot \hat{\mathbf{u}} = 0, \quad (2.3)$$

$$\rho_0 \frac{\partial \hat{\mathbf{u}}}{\partial \hat{t}} + \nabla \hat{p} = 0. \quad (2.4)$$

The next step is to transform these equations to frequency domain and assuming only wave propagation in the x -direction, integrating over the cross section we find:

$$\frac{i\omega}{c_0^2} p + \frac{\rho_0}{S_f} \frac{dU}{dx} = 0, \quad (2.5)$$

$$\rho_0 i\omega U + S_f \frac{dp}{dx} = 0, \quad (2.6)$$

where U denotes the acoustic volume flow in $\text{m}^3 \cdot \text{s}^{-1}$. Eqs. (2.5-2.6) is a coupled set of ordinary differential equations, which can be solved for the acoustic pressure to find

$$p(x) = A \exp(-ikx) + B \exp(ikx), \quad (2.7)$$

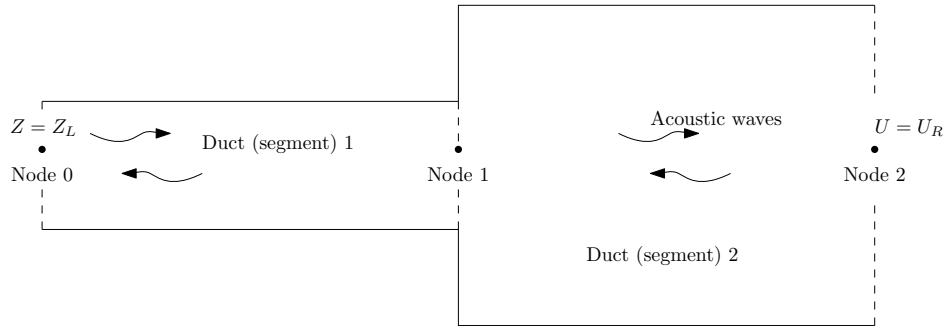


Figure 2.1 – Example of two simple duct segments connected together.

where A and B are constants, to be determined from the boundary conditions. Setting $p = p_L$, and $U = U_L$ at $x = 0$, we can solve for the acoustic pressure, upon using Eq. 2.6 as:

$$p(x) = p_L \cos(kx) - iZ_0 \sin(kx) U_L, \quad (2.8)$$

and for the acoustic volume flow we find:

$$U(x) = U_L \cos(kx) - \frac{i}{Z_0} \sin(kx) p_L. \quad (2.9)$$

Now, we have all ingredients to derive the transfer matrix of an acoustic duct. Setting $p(x = L) = p_R$, and $U(x = L) = U_R$, we find the following two-port coupling between the pressure and the velocity from the left side of the duct to the right side of the duct:

$$\begin{Bmatrix} p_R \\ U_R \end{Bmatrix} = \begin{bmatrix} \cos(kL) & -iZ_0 \sin(kL) \\ -iZ_0^{-1} \sin(kL) & \cos(kL) \end{bmatrix} \begin{Bmatrix} p_L \\ U_L \end{Bmatrix}. \quad (2.10)$$

2.3 Setting up the system of equations

LRFTubes has been set up to solve systems of acoustic segments such as this prismatic duct. The advantage of the transfer matrix method is the ease with which mixed (impedance/pressure/velocity) boundary conditions can be implemented.

In this section, the assembly of the global system of equations is explained. The state variables of each segment are stacked in a column vector ϕ_{sys} , which has the size of $4N_{\text{segs}}$, where N_{segs} denotes the number of segments in the system. The coupling equations between the nodes of each segment, are the transfer matrices. Since the transfer matrices are 2×2 , this fills only half of the required amount of equations. The other half is filled with boundary conditions. Each segments transfer matrix can be regarded as the element matrix, which all have a form like:

$$\phi_R = T \cdot \phi_L + s, \quad (2.11)$$

where ϕ_L , ϕ_R are the state vectors on the left and right sides of the segment, respectively, T is the transfer matrix, and s is a source term.

There are two kind of boundary conditions, called external and internal boundary conditions. External boundary conditions apply where a prescribed condition is given, such as a prescribed pressure, voltage, volume flow, current or acoustic/electric impedance. Internal boundary conditions are used to couple different segments at a connection point, which is recognized by a shared node number. At a connection point, the effort variable is shared, which means that the pressure at the node is equal for each connected segment sharing the node. The flow variable is conserved, so the sum of the volume flow out of all segments connected at the node is 0.

Example: two ducts

This procedure of creating a system matrix is explained by an example where only two ducts are coupled. A schematic of the situation is depicted in Figure 2.1. For the example situation, at the left node of segment

(1), an impedance boundary Z_L is prescribed. The right node of segment (1) is connected to the left node of segment (2), and at the right side of segment (2), a volume flow boundary condition is prescribed of U_R . The corresponding system of equations for this case is

$$\left[\begin{array}{cccc}
 \mathbf{T}_1 & -\mathbf{I} & \mathbf{0} & \mathbf{0} \\
 \mathbf{0} & \mathbf{0} & \mathbf{T}_2 & -\mathbf{I} \\
 \mathbf{0} & \begin{bmatrix} 1 & 0 \\ 0 & 1 \end{bmatrix} & \begin{bmatrix} -1 & 0 \\ 0 & -1 \end{bmatrix} & \mathbf{0} \\
 \begin{bmatrix} 1 & Z_L \\ 0 & 0 \end{bmatrix} & \mathbf{0} & \mathbf{0} & \begin{bmatrix} 0 & 0 \\ 0 & 1 \end{bmatrix}
 \end{array} \right] \left\{ \begin{array}{l} p_{1L} \\ U_{1L} \\ p_{1R} \\ U_{1R} \\ p_{2L} \\ U_{2L} \\ p_{2R} \\ U_{2R} \end{array} \right\} = \left\{ \begin{array}{l} 0 \\ 0 \\ 0 \\ 0 \\ 0 \\ 0 \\ 0 \\ U_R \end{array} \right\}, \quad (2.12)$$

In this system matrix, $\mathbf{0}$ denotes a 2×2 sub matrix of zeros and \mathbf{I} denotes a 2×2 identity sub matrix. \mathbf{T}_i is the transfer matrix of the i -th segment. The solution can be obtained by Gaussian elimination, for which in **LRFTubes** the `numpy.linalg.solve()` solver is used. Once the solution on the nodes is known, the solution in each segment can be computed as a post processing step. **LRFTubes** provides some post processing routines to aid in visualization of the acoustic field inside a non-lumped segment, such as an acoustic duct.

Chapter 3

Provided acoustic models

3.1 Introduction

This chapter provides a concise overview of the provided acoustic models implemented in **LRFTubes**.

3.2 Prismatic duct

A prismatic duct is used to model one-dimensional acoustic wave propagation. The prismatic duct is implemented in **LRFTubes** in the `PrSDuct` class. Figure 3.1 shows this segment schematically. In the thermal boundary layer, heat and momentum diffuse to the wall. The thermal boundary layer can be a small layer w.r.t. to the transverse characteristic length scale of the tube, or can fully occupy the tube. In the latter case, the solution converges to the classic laminar Poiseuille flow solution. The basic assumptions behind this model are

- Prismatic cross sectional area.
- $L \gg r_h$, (tube is long compared to its transverse length scale).
- Radius is much smaller than the wave length.
- Wave length is much larger than viscous penetration depth.
- End effects and entrance effects are negligible.

For a formal derivation of the model for prismatic cylindrical tubes, the reader is referred to the work of Tijdeman [10] and Nijhof [6]. For a somewhat more pragmatic derivation, we would like to refer to the work of Swift [9, 8] and Rott [7].

$$\frac{dp}{dx} = \frac{\omega \rho_0}{i(1-f_v)S_f} U, \quad (3.1)$$
$$\frac{dU}{dx} = \frac{k}{iZ_0} \left(1 + \frac{(\gamma-1)f_k}{1+\epsilon_s}\right) p, \quad (3.2)$$

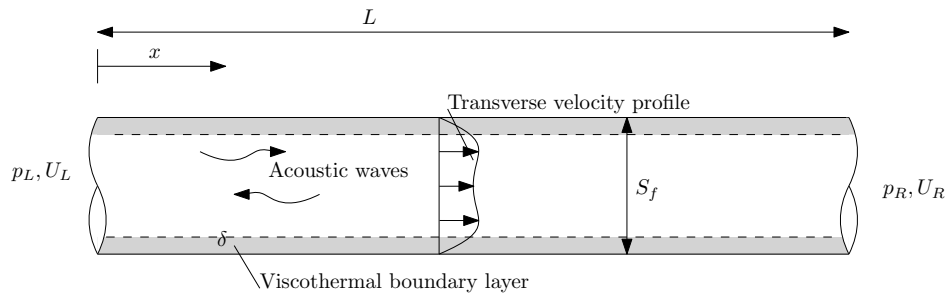


Figure 3.1 – Geometry of the prismatic duct

where S_f is the cross-sectional area filled with fluid, k is the inviscid wave number, and Z_0 the inviscid characteristic impedance of a tube ($Z_0 = z_0/S_f$). f_v and f_κ are the viscous and thermal Rott functions, respectively [7]. They model the viscous and thermal effects with the wall. For circular tubes, the f 's are defined as [9, p. 88]:

$$f_{j,\text{circ}} = \frac{J_1 \left[(i-1) \frac{2r_h}{\delta_j} \right]}{(i-1) \frac{r_h}{\delta} J_0 \left[(i-1) \frac{2r_h}{\delta_j} \right]}, \quad (3.3)$$

where $\delta_j = \delta_v$ for $f_{v,\text{circ}}$ and $\delta_j = \delta_\kappa$ for $f_{\kappa,\text{circ}}$. J_α denotes the cylindrical Bessel function of the first kind and order α . r_h is the hydraulic radius, defined as the ratio of the cross sectional area to the ‘‘wetted perimeter’’:

$$r_h = S_f / \Pi. \quad (3.4)$$

Note that for a circular tube with diameter D , $r_h = D/4$. The parameter ϵ_s in Eq. 3.2 is the ideal solid correction factor, which corrects for solids that have a finite heat capacity. This parameter is dependent on the thermal properties and the geometry of the solid. An example of ϵ_s is derived in Section A.1. For the case of an thermally ideal solid, ϵ_s can be set to 0.

Upon solving for Eqs. 3.1-3.2, a transfer matrix can be derived which couples the pressure and volume flow on the left side to the right side as:

$$\begin{Bmatrix} p_R \\ U_R \end{Bmatrix} = \begin{bmatrix} \cos(\Gamma L) & -iZ_c \sin(\Gamma L) \\ -iZ_c^{-1} \sin(\Gamma L) & \cos(\Gamma L) \end{bmatrix} \begin{Bmatrix} p_L \\ U_L \end{Bmatrix}, \quad (3.5)$$

where Z_c is the characteristic impedance of the duct, i.e. the impedance p/U of a plane (although damped) propagating wave:

$$Z_c = \frac{kZ_0}{(1-f_v)\Gamma}. \quad (3.6)$$

The parameter Γ in Eqs. 3.5 and 3.6 is the viscothermal wave number, i.e. the wave number corrected for viscothermal losses:

$$\Gamma = k \sqrt{\frac{1 + \frac{(y-1)f_\kappa}{1+\epsilon_s}}{1-f_v}}. \quad (3.7)$$

Due to the numerical implementation of the Bessel functions in many libraries, the f_j function for cylindrical ducts (Eq. 3.3) cannot be computed for high r_h/δ by computing this ratio J_1/J_0 . The numerical result starts to break down at $r_h/\delta \sim 100$. To resolve this problem, the **LRFTubes** code applies a smooth transition from the Bessel function ratio to the boundary layer limit solution for f :

$$f_{j,\text{bl}} = \frac{(1-i)\delta_j}{2r_h} \quad (3.8)$$

in the range of $100 < r_h/\delta \leq 200$.

Note that in the limit of $r_h \rightarrow \infty$, or κ and $\mu \rightarrow 0$, $\Re[\Gamma] \rightarrow k$ and $\Re[Z_c] \rightarrow Z_0$ whereas $\Im[\Gamma]$ and $\Im[Z_c] \rightarrow 0$. Hence in these limits the lossless wave equation is resolved from the result. This is not true in the limit of $\omega \rightarrow \infty$, as in that limit it can be computed that $\Re[\Gamma] \rightarrow k$, while the imaginary part

$$-\Im[\Gamma] \rightarrow \sqrt{\omega} \frac{\sqrt{\frac{1}{8} \frac{\mu}{\rho_0}}}{c_0 r_h} \left[1 + \frac{(y-1)}{\sqrt{\text{Pr}}} \right]. \quad (3.9)$$

In other words the imaginary part of the wave number keeps growing, although with a smaller rate than real part of the wave number. So the higher the frequency, the smaller the viscothermal damping per wavelength, but the higher the viscothermal damping per meter of duct.

Figure 3.2 shows the imaginary part of the wave number as a function of the frequency. As visible, the magnitude of the viscothermal damping grows monotonically with frequency.

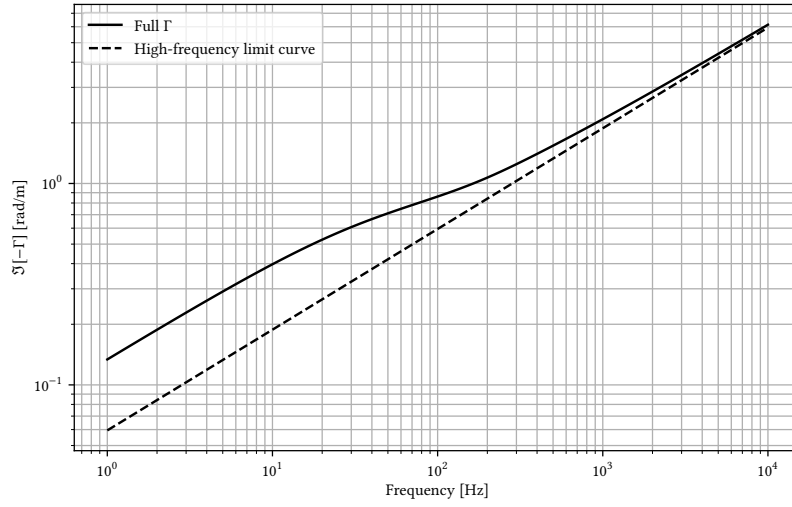


Figure 3.2 – Logarithmic plot of the negative of imaginary part of the viscothermal wave number ($-\Im[\Gamma]$), for a tube with a diameter of 1 mm. In blue, the full f_v and f_κ of Eq. 3.7 and 3.3 is used. The orange curve corresponds to Eq. 3.9.

3.3 Prismatic lined circular duct

The Fourier transformed wave equation in axisymmetric cylindrical coordinates can be written as:

$$\frac{\partial^2 p}{\partial r^2} + \frac{1}{r} \frac{\partial p}{\partial r} + \frac{\partial^2 p}{\partial x^2} + k^2 p = 0, \quad (3.10)$$

Using separation of variables:

$$p = \rho(r)\xi(x), \quad (3.11)$$

this can be written as:

$$\frac{\rho''}{\rho} + \frac{1}{r} \frac{\rho'}{\rho} + \frac{\xi''}{\xi} + k^2 = 0 \quad (3.12)$$

Solutions:

$$\xi = \exp(-i\alpha x), \quad (3.13)$$

$$\rho = J_0(\epsilon r), \quad (3.14)$$

such that the solution for the pressure is:

$$p = J_0(\epsilon r) \exp(\alpha x) \quad (3.15)$$

under the condition:

$$\alpha^2 = k^2 - \epsilon^2. \quad (3.16)$$

At $r = R$ we have the boundary condition that $Z_0 \zeta_R u = p$. After filling in and using the rule $J_0'(x) = -J_1(x)$:

$$\epsilon R \frac{J_1(\epsilon R)}{J_0(\epsilon R)} = -iv, \quad (3.17)$$

where $v = \frac{kR}{\zeta R}$. This is the characteristic equation for ϵR . Solutions for

$$\epsilon \approx + \frac{1}{R} \sqrt{\frac{96 + 36iv \pm \sqrt{9216 + 2304iv - 912v^2}}{12 + iv}} \quad (3.18)$$

where $0 \leq \Re[\epsilon R] \leq 2$ and $0 \leq \Im[\epsilon R] \leq 3$ should be satisfied in order to guarantee precision, see Mechel, p. 630.

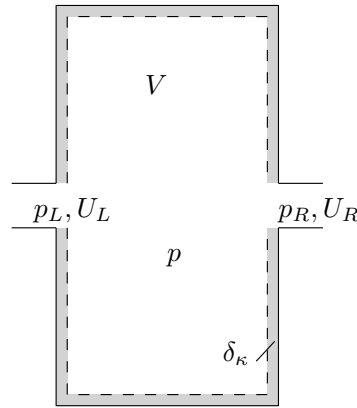


Figure 3.3 – Schematic of the compliance volume segment.

3.3.1 Cremers impedance

$$\frac{kR}{\zeta} = 2.9803824 + 1.2796025i \quad (3.19)$$

Or:

$$\zeta = kR(0.28 - 0.12i) \quad (3.20)$$

Attenuation reached when the liner impedance equals Cremer's impedance is around 15 dB per unit of radius maximum. It decreases with increasing frequency, when $fR \approx 100$.

3.3.2 Locally reacting lining with back-volume

Impedance of concentric liner, outer radius is R_o , inner radius is R_i

$$\zeta_{\text{back}} = i \frac{H_0^{(1)}(kR_i) - \frac{H_1^{(1)}(kR_o)}{H_1^{(2)}(kR_o)} H_0^{(2)}(kR_i)}{H_1^{(1)}(kR_i) - \frac{H_1^{(1)}(kR_o)}{H_1^{(2)}(kR_o)} H_1^{(2)}(kR_i)} \quad (3.21)$$

Such that the total impedance is

$$\zeta = \zeta_{\text{back}} + \zeta_{\text{MPP}} \quad (3.22)$$

3.4 Compliance volume

Figure 3.3 gives a schematic of the compliance volume. A compliance volume is implemented in the **LRF-Tubes** code in the `Volume` class. A compliance volume is a volume (tank) which is small compared to the wavelength. Hence, we can assume that the acoustic pressure is constant throughout the volume V . As thermal relaxation still occurs, the model for this segment takes into account thermal relaxation due to temperature oscillations. The basic assumptions behind the model are:

- The characteristic length scale of volume is small compared to the wavelength.
- The characteristic length scale of volume is large compared to thermal penetration depth.

The lower the frequency, the more the second assumption is violated, while the higher the frequency, the more the first assumption is violated. In practice, violating the first assumption has a larger impact. For a compliance, the following governing equations can be derived [11, p. 156]:

$$p_L = p = p_R, \quad (3.23)$$

$$U_R = U_L - i\omega C_c p, \quad (3.24)$$

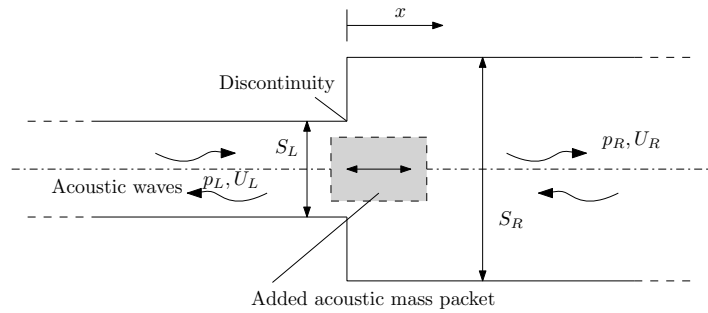


Figure 3.4 – Schematic of a waveguide discontinuity.

in which C_c is the acoustic “capacitance”:

$$C_c = \frac{1}{z_0 c_0} \left(V + \frac{1(1-i)(\gamma-1)}{2(1+\epsilon_{s,0})} S \delta_\kappa \right) \quad (3.25)$$

where V is the volume, S the surface area of the volume in contact with a wall, and

$$\epsilon_{s,0} = \sqrt{\frac{\kappa \rho_0 c_p}{\kappa_s \rho_s c_s}}. \quad (3.26)$$

It should be noticed that in practice, a compliance volume often functions as the end of an acoustic system. In that case, either U_L or U_R is 0.

3.5 End corrections and discontinuities

For discontinuities in the cross section of a waveguide, and the case of inviscid adiabatic wave propagation, an exact expression is available for the added acoustic mass [5]. Figure 3.4 gives a schematic of the situation. The model is implemented in the `Discontinuity` class in the **LRFTubes** code. The assumptions behind the model are:

- Both tubes on either side of the discontinuity are cylindrical. The tubes are co-axially connected.
- The wavelength is larger than transverse characteristic length scale.
- Other discontinuities are far away from the current one.
- Inviscid and adiabatic wave propagation (Helmholtz equation).

The ratio of tube radii a_L/a_R is denoted by α . It turns out that a surface area discontinuity only generates an acoustic pressure discontinuity. The volume flow is preserved. Hence:

$$U_R = U_L \quad (3.27)$$

$$p_R = p_L - i\omega M_A U_L \quad (3.28)$$

where M_A is the so-called added acoustic mass in $\text{kg} \cdot \text{m}^{-4}$, which equals

$$M_A = \chi(\alpha, k) \frac{8\rho_0}{3\pi^2 a_L}, \quad (3.29)$$

where χ is Karal’s discontinuity factor, which is in general a function of the tube radii and the wave number.

For $\lambda \gg a_R$, the dependency of χ on the wave number k can be neglected, which lowers the computational burden significantly, as χ has to be computed only once. For the case $\alpha \rightarrow 0$ (by letting $a_R \rightarrow \infty$), $\chi \rightarrow 1$. In case of $\alpha \rightarrow 1$, the acoustic mass gradually reduces to zero as $\chi \rightarrow 0$. When $\alpha = 1$, there is no continuity left, such that $M_A = 0$.

The derivation of the coefficient χ is documented in Appendix B, except of the following information. To solve the curve of χ , a system of infinite equations has to be solved for an infinite number of unknowns. In the

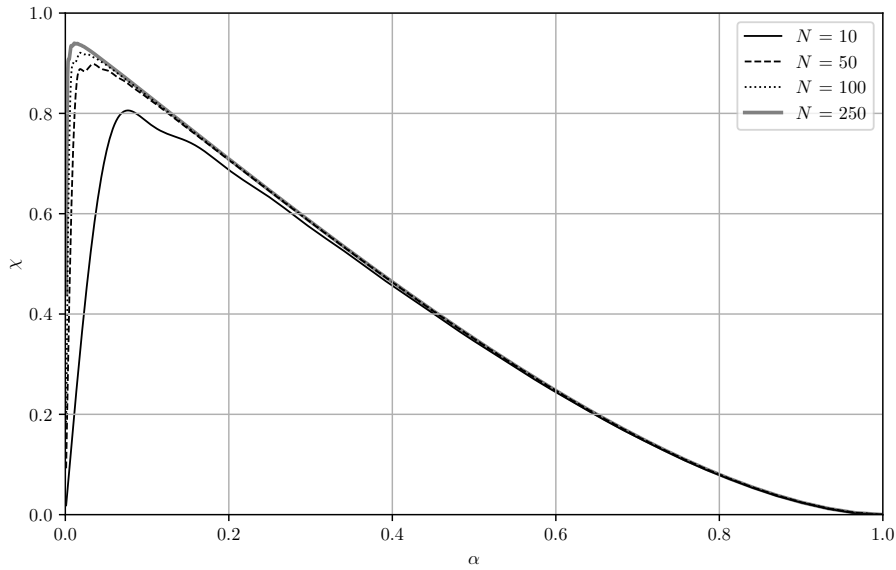


Figure 3.5 – χ vs α for different truncations (N) of the infinite system of equations.

LRFTubes code, as a standard this system is truncated up to $N = 100$ equations and 100 unknowns. Figure 3.5 shows the effect of truncating this infinite system of equations. As visible for the case of 100 equations, the curves start to deviate from each other for lower values of α . Assuming that convergence is obtained as $N \rightarrow \infty$, the curve of $N = 100$ has acceptable accuracy for $\alpha > 0.07$. To limit possible faulty results, the **LRFTubes** code gives a warning when the tube ratio is chosen such that an invalid χ is computed. When an $\alpha < 0.07$ is desired, the user should choose a higher value of N .

3.6 Hard wall

A hard wall is the wall perpendicular to the wave propagation direction. Figure 3.6 shows the schematic configuration for this segment. Due to thermal relaxation a hard wall consumes acoustic energy is consumed. The hard wall segment models this thermal relaxation loss. The assumptions behind the model are:

- Normal incident waves.
- Uniform normal velocity.
- The wavelength is much larger than the thermal penetration depth ($\lambda \gg \delta_\kappa$).

We can derive the following impedance boundary condition [11, p. 157]:

$$U = k\delta_\kappa \frac{S}{z_0} \frac{(\gamma - 1)(1 + i)}{2(1 + \epsilon_s)} p. \quad (3.30)$$

Hence the impedance of a hard wall scales with $Z \sim Z_0 \frac{\lambda}{\delta_\kappa}$. For 1 kHz, this results in $\sim 4100Z_0$, which is practically already close to ∞ . Except for really high frequencies this segment can often be replaced with a boundary condition of $U = 0$. An important point to make here is that this boundary condition is inconsistent with the LRF solution for 1D wave propagation in ducts, as the velocity profile in a duct is not uniform. This is especially true for the case of small ducts where $r_h \sim \delta$.

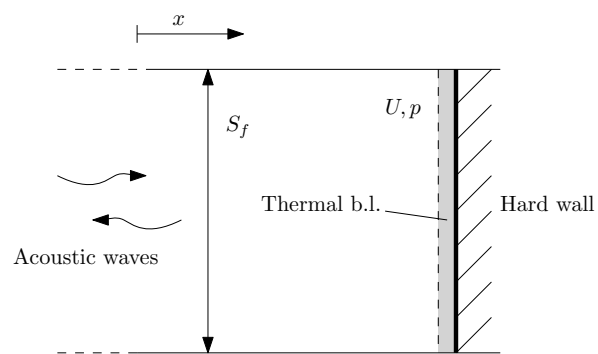


Figure 3.6 – Schematic of a hard acoustic wall where the thermal boundary layer dissipates a bit of the acoustic energy ($Z \neq \infty$).

Bibliography

- [1] D. Blackstock. *Fundamentals of physical acoustics*. Hoboken, NJ, USA: John Wiley & Sons, 2000. 541 pp.
- [2] J. De Jong. “Numerical modeling of thermoacoustic systems.” PhD thesis. Enschede: Universiteit Twente, 2015.
- [3] F. van der Eerden. “Noise reduction with coupled prismatic tubes.” PhD thesis. Enschede, The Netherlands: University of Twente, Nov. 2000.
- [4] W. Kampinga. “Viscothermal acoustics using finite elements: analysis tools for engineers.” PhD thesis. Enschede, The Netherlands: University of Twente, 2010.
- [5] F. Karal. “The analogous acoustical impedance for discontinuities and constrictions of circular cross section.” *The Journal of the Acoustical Society of America* 25.2 (1953), pp. 327–334.
- [6] M. J. J. Nijhof. “Viscothermal wave propagation.” PhD thesis. E: University of Twente, 2010.
- [7] N. Rott. “Damped and thermally driven acoustic oscillations in wide and narrow tubes.” *Zeitschrift für angewandte Mathematik und Physik* 20.2 (Mar. 1969), pp. 230–243.
- [8] G. W. Swift. “Thermoacoustic Engines.” *The Journal of the Acoustical Society of America* 84.4 (1988), pp. 1145–1180.
- [9] G. W. Swift. *Thermoacoustics: A unifying perspective for some engines and refrigerators*. Melville, NY, USA: Acoustical Society of America, 2003. 315 pp.
- [10] H. Tijdeman. “On the propagation of sound waves in cylindrical tubes.” *Journal of Sound and Vibration* 39.1 (Mar. 8, 1975), pp. 1–33.
- [11] W. C. Ward, J. P. Clark, and G. W. Swift. *DeltaEC Users Guide version 6.4b2.7*. Dec. 4, 2017.

Appendix A

Thermal relaxation in thick tubes

A.1 Thermal relaxation effect in thick tubes

In this section, a formulation for ϵ_s is given for tubes where the temperature wave in the solid is present. Figure A.1 shows a schematic overview of the situation. As shown in the figure, the temperature wave accompanied with an acoustic wave results in heat conduction to/from the wall of the tube. To solve this interaction mathematically, the heat equation in the solid has to be solved. For constant thermal conductivity, density and heat capacity the heat equation of the solid is

$$\rho_s c_s \frac{\partial \tilde{T}_s}{\partial t} = \kappa_s \nabla^2 \tilde{T}_s, \quad (\text{A.1})$$

where ρ_s , c_s , \tilde{T}_s and κ_s are the density, specific heat, temperature and thermal conductivity of the solid, respectively. In frequency domain and using cylindrical coordinates, assuming axial symmetry, this can be written as

$$\left(r^2 \left(\frac{\partial^2}{\partial r^2} + \frac{\partial^2}{\partial x^2} \right) + r \frac{\partial}{\partial r} + \frac{2}{i\delta_s^2} r^2 \right) T_s = 0, \quad (\text{A.2})$$

where δ_s is

$$\delta_s = \sqrt{\frac{2\kappa_s}{\rho_s c_s \omega}}. \quad (\text{A.3})$$

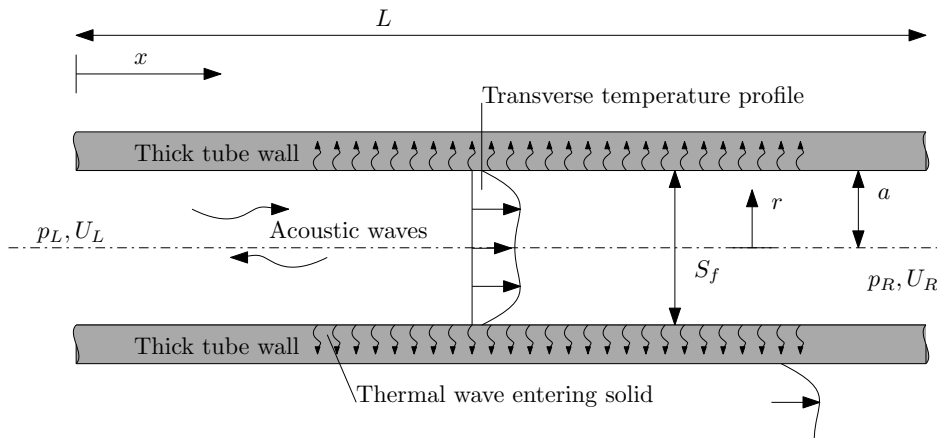


Figure A.1 – Schematic situation of a tube surrounded by a thick solid. Note that the transverse acoustic temperature is drawn to be not zero at the wall. This happens in case of thermal interaction with a solid with finite thermal effusivity.

Now, since $\partial T_s / \partial x \sim \frac{\delta_s}{\lambda} \frac{\partial T_s}{\partial r}$, the second order derivative of the temperature in the axial direction can be neglected. In that case, the differential equation to solve for is

$$\left(r^2 \frac{\partial^2}{\partial r^2} + r \frac{\partial}{\partial r} + \frac{2}{i\delta_s^2} r^2 \right) T_s = 0, \quad (\text{A.4})$$

which is a Bessel differential equation of the zero'th order in T_s . The solutions is sought in terms of traveling cylindrical waves:

$$T_s = C_1 H_0^{(1)} \left((i-1) \frac{r}{\delta_s} \right) + C_2 H_0^{(2)} \left((i-1) \frac{r}{\delta_s} \right), \quad (\text{A.5})$$

where C_1 and C_2 constants to be determined from the boundary conditions, and $H_\alpha^{(i)}$ is the cylindrical Hankel function of the $(i)^{\text{th}}$ kind and order α . If we require $T_s \rightarrow 0$ as $r \rightarrow \infty$, the constant C_2 is required to be 0. From the acoustic energy equation, a similar differential equation can be found for the acoustic temperature in the fluid:

$$\left(r^2 \frac{\partial^2}{\partial r^2} + r \frac{\partial}{\partial r} + \frac{2}{i\delta_s^2} r^2 \right) T = \frac{2}{i\delta_s^2} \frac{\alpha_p T_0}{\rho_0 c_p} p,$$

for which the (partial) solution is

$$T = \frac{\alpha_p T_0}{\rho_0 c_p} p \left(1 - C_3 J_0 \left((i-1) \frac{r}{\delta_\kappa} \right) \right). \quad (\text{A.6})$$

To attain at Eq. A.6, use has been made of the fact that the temperature should be finite at $r = 0$. C_3 is a constant that is to be determined from the boundary conditions at the solid-fluid interface. These boundary conditions are:

$$T_s|_{r=a} = T|_{r=a}, \quad (\text{A.7})$$

$$-\kappa_s \frac{\partial T_s}{\partial r} |_{r=a} = -\kappa \frac{\partial T}{\partial r} |_{r=a}, \quad (\text{A.8})$$

i.e. continuity of the temperature and the heat flux at the interface. This yields two equations for two unknowns (C_1 and C_3 , C_2 is already argued to be 0). Solving for the acoustic temperature yields:

$$T = \frac{\alpha_p T_0}{\rho_0 c_p} p \left(1 - \frac{1}{(1 + \epsilon_s)} \frac{J_0 \left((i-1) \frac{r}{\delta_\kappa} \right)}{J_0 \left((i-1) \frac{a}{\delta_\kappa} \right)} \right),$$

where

$$\epsilon_s = \frac{e_f J_1 \left((i-1) \frac{a}{\delta_\kappa} \right) H_0^{(1)} \left((i-1) \frac{a}{\delta_s} \right)}{e_s J_0 \left((i-1) \frac{a}{\delta_\kappa} \right) H_1^{(1)} \left((i-1) \frac{a}{\delta_s} \right)}, \quad (\text{A.9})$$

where e_f is the thermal effusivity of the fluid, and e_s the thermal effusivity of the solid, such that the ratio is

$$\frac{e_f}{e_s} = \sqrt{\frac{\kappa \rho_0 c_p}{\kappa_s \rho_s c_s}}. \quad (\text{A.10})$$

Note that for large a/δ_κ :

$$\frac{J_1 \left((i-1) \frac{a}{\delta_\kappa} \right)}{J_0 \left((i-1) \frac{a}{\delta_\kappa} \right)} \rightarrow i, \quad (\text{A.11})$$

and for large a/δ_s

$$\frac{H_0^{(1)} \left((i-1) \frac{a}{\delta_s} \right)}{H_1^{(1)} \left((i-1) \frac{a}{\delta_s} \right)} \rightarrow -i, \quad (\text{A.12})$$

such that for both numbers large

$$\epsilon_s \rightarrow \frac{e_f}{e_s}. \quad (\text{A.13})$$

Appendix B

Derivation of Karal's discontinuity factor

Note: this documentation is incomplete.

This appendix describes the derivation of Karal's discontinuity factor. The following assumptions underlie the model:

- $z = 0$: position of the discontinuity
- Assume $f \ll f_c$, such that far away from the discontinuity, only propagating modes exist.
- Assume axial symmetry, so dependence of θ is dropped

In cylindrical coordinates, the solution of the Helmholtz equation can be written in terms of cylindrical harmonics [1]. Assuming axial symmetry such that the acoustic pressure in for example tube B can be written as:

$$p_B = \begin{Bmatrix} J_m(k_r r) \\ N_m(k_r r) \end{Bmatrix} \begin{Bmatrix} e^{im\phi} \\ e^{-im\phi} \end{Bmatrix} \begin{Bmatrix} e^{\beta z} \\ e^{-\beta z} \end{Bmatrix} \quad (\text{B.1})$$

where J_m is the cylindrical Bessel function of order

$$k_r^2 - \beta^2 = k^2. \quad (\text{B.2})$$

Using the boundary condition that

$$\frac{\partial p_B}{\partial r} \Big|_{r=b} = 0, \quad (\text{B.3})$$

and assuming axial symmetry (only the $m = 0$ modes) it follows that

$$\frac{\partial J_0}{\partial r}(k_r b) \Big|_{r=b} = 0. \quad (\text{B.4})$$

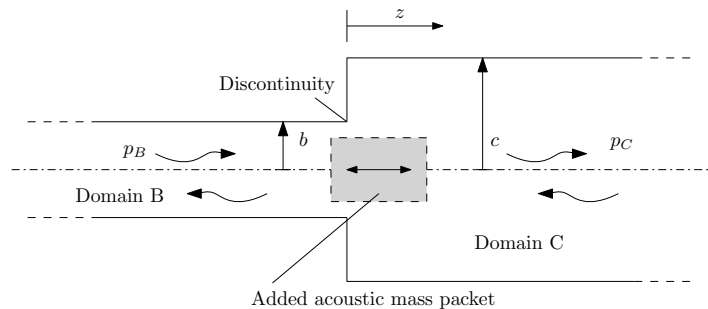


Figure B.1 – Schematic of a discontinuity at the interface between two tubes with different radius. Domain B is the smaller tube and domain C is the larger tube. The radius of the tube in domain B is b , and the radius of the tube in domain C is c .

Assuming that α_k is the k^{th} zero of $J_0'(x)$, we can write for $k_{r,k}$:

$$k_{r,k} = \frac{\alpha_k}{b}. \quad (\text{B.5})$$

Hence we find the following reduced expression for the pressure in tube B:

$$p_B = B_0^0 \exp(ikz) + B_0^1 \exp(-ikz) + \sum_{n=1}^{\infty} B_n J_0\left(\alpha_n \frac{r}{b}\right) \left\{ \begin{array}{l} e^{\beta_n z} \\ e^{-\beta_n z} \end{array} \right\}, \quad (\text{B.6})$$

where accordingly,

$$\beta_k^2 = \left(\frac{\alpha_k}{b}\right)^2 - k^2 \quad (\text{B.7})$$

For $k^2 < (\alpha_k/b)^2$, $\beta_k^2 > 0$, the modes are evanescent. And since we only allow finite solutions for $z \leq 0$, the final results for p_B is

$$p_B = B_0^0 \exp(ikz) + B_0^1 \exp(-ikz) + \sum_{n=1}^{\infty} B_n J_0\left(\alpha_n \frac{r}{b}\right) e^{\beta_n z}, \quad (\text{B.8})$$

where β_n is defined as the positive root of the r.h.s. of Eq. B.7. We simplify this relation to:

$$p_B(z) = p_B^0(z) + \sum_{n=1}^{\infty} B_n J_0\left(\alpha_n \frac{r}{b}\right) e^{\beta_n z}. \quad (\text{B.9})$$

For the velocity we find

$$u_B(z) = u_B^0(z) + \sum_{n=1}^{\infty} Y_{B,n} B_n J_0\left(\alpha_n \frac{r}{b}\right) e^{\beta_n z}, \quad (\text{B.10})$$

where

$$Y_{B,n} = \frac{i\beta_n}{\omega\rho_0}. \quad (\text{B.11})$$

Similarly, for the positive z we find

$$p_C(z) = P_C^0(z) + \sum_{m=1}^{\infty} C_m J_0\left(\alpha_m \frac{r}{c}\right) e^{-\gamma_m z}, \quad (\text{B.12})$$

where

$$\gamma_m = \sqrt{\left(\frac{\alpha_m}{c}\right)^2 - k^2}. \quad (\text{B.13})$$

and

$$u_C(z) = u_C^0(z) + \sum_{m=1}^{\infty} Y_{C,m} C_m J_0\left(\alpha_m \frac{r}{c}\right) e^{-\gamma_m z}, \quad (\text{B.14})$$

where

$$Y_{C,m} = -\frac{i\gamma_m}{\omega\rho_0} \quad (\text{B.15})$$

B.1 Boundary conditions

At the interface ($z = 0$), the following boundary conditions are valid:

$$u_B|_{z=0} = u_C|_{z=0} \quad 0 \leq r \leq b \quad (\text{B.16})$$

$$u_C|_{z=0} = 0 \quad b \leq r \leq c \quad (\text{B.17})$$

$$p_B = p_C \quad 0 \leq r \leq b \quad (\text{B.18})$$

Taking Eq. B.16, multiply by r and integrating from 0 to c , taking into account Eq. B.17 yields:

$$b^2 u_B^0 = c^2 u_C^0 \quad (\text{B.19})$$

We require one more equation at the interface, which is found from the continuity boundary conditions as well. Multiplying Eq. B.16 with $J_0(\alpha_q \frac{r}{c})r$ and integrating setting $q = m$ and dividing by bc yields:

$$u_B^0 J_1(\alpha_m \rho) \frac{1}{\alpha_q} + \sum_{n=1}^{\infty} Y_{B,n} T_{mn} B_n = Y_{C,m} \frac{1}{2} \rho^{-1} J_0(\alpha_m)^2 C_m, \quad (\text{B.20})$$

where

$$T_{mn} = \frac{\alpha_m}{\alpha_m^2 - \frac{\alpha_n^2}{\rho^2}} J_0(\alpha_n) J_1(\alpha_m \rho). \quad (\text{B.21})$$

Setting $p_B = p_C$

$$p_B^0 = p_C^0 + 2 \sum_{m=1}^{\infty} \frac{J_1(\alpha_m \rho)}{\rho \alpha_m} C_m \quad (\text{B.22})$$

$$B_n J_0(\alpha_n)^2 = \frac{2}{\rho} \sum_{m=1}^{\infty} T_{mn} C_m \quad (\text{B.23})$$

$$\sum_{n=1}^{\infty} \frac{2\alpha_n}{J_0(\alpha_n)^2} T_{mn} \sum_{q=1}^{\infty} T_{qn} D_q + \frac{1}{2} \rho \alpha_m J_0(\alpha_m)^2 D_m = J_1(\alpha_m \rho) \frac{\rho}{\alpha_m}, \quad (\text{B.24})$$

where

$$D_m = \frac{C_m}{ikb u_B^0 z_0} \quad (\text{B.25})$$

Eq. B.24 is a set of infinite equations in terms of an infinite number of unknowns for D_m . In matrix algebra for a finite set, this can be written as

$$(\mathbf{M}_1 \cdot \mathbf{M}_2 + \mathbf{K}) \cdot \mathbf{D} = \mathbf{R} \quad (\text{B.26})$$

where

$$M_{1,ij} = \frac{2\alpha_j}{J_0(\alpha_j)^2} T_{ij} \quad (\text{B.27})$$

$$M_{2,ij} = T_{ji} \quad (\text{B.28})$$

$$K_{ij} = \frac{1}{2} \rho \alpha_j J_0(\alpha_j)^2 \quad ; \quad i = j \quad (\text{B.29})$$

$$K_{ij} = 0 \quad ; \quad i \neq j \quad (\text{B.30})$$

$$R_i = J_1(\alpha_i \rho) \frac{\rho}{\alpha_q} \quad (\text{B.31})$$

Finally, the added acoustic mass,

$$p_C^0 = p_B^0 - i\omega M_A U_B, \quad (\text{B.32})$$

can be computed as

$$\rho_0 \sum_{m=1}^{\infty} \frac{2}{\pi b} \frac{J_1(\alpha_m \rho)}{\rho \alpha_m} D_m \quad (\text{B.33})$$

For a given velocity $u_{C,0}$ the velocity profile at $z = 0$ is

$$u_C = u_C^0 + bu_B^0 \sum_{m=1}^{\infty} \gamma_m D_m J_0\left(\alpha_m \frac{r}{c}\right) \quad (\text{B.34})$$